Astron. Astrophys. 359, 419–428 (2000)

ASTRONOMY AND ASTROPHYSICS

Constraints on the cosmic infra-red background based on BeppoSAX and CAT spectra of Markarian 501

J. Guy[1], **C. Renault**[1], **F.A. Aharonian**[2], **M. Rivoal**[1], **and J.-P. Tavernet**[1]

[1] LPNHE, CNRS-IN2P3 Universités Paris VI-VII, 4 place Jussieu, 75252 Paris Cedex 05, France
[2] Max-Planck-Institut für Kernphysik, Postfach 103980, 69029 Heidelberg, Germany

Received 24 November 1999 / Accepted 26 April 2000

Abstract. The TeV and X-ray data obtained by the imaging Cherenkov telescope CAT and X-ray satellite BeppoSAX during the remarkable flare of Mkn 501 in April 16, 1997 are used to constrain the flux of the Cosmic Infrared Background (CIB) using different CIB models. We show that a non-negligible absorption of γ-rays due to the CIB could take place already in the low-energy (sub-TeV) domain of the spectrum of Mkn 501. This implies that the data of the low-energy threshold CAT telescope contain very important information about the CIB at short wavelengths, 0.4 μm$\leq \lambda \leq 3.$ μm. The analysis of almost simultaneous spectroscopic measurements of Mkn 501 in a high state by CAT and BeppoSAX in the framework of the standard homogeneous Synchrotron-Self-Compton (SSC) framework model leads to the conclusion that the density of the near-infrared background with typical "starlight spectrum" around 1 μm should be between 5 and $35\,\mathrm{nW\,m^{-2}\,sr^{-1}}$ (99% CL), with most likely value around $20\,\mathrm{nW\,m^{-2}\,sr^{-1}}$. Also we argue that the CAT γ-ray data alone allow rather robust upper limits on the CIB, $\lambda F_\lambda \leq 60\,\mathrm{nW\,m^{-2}\,sr^{-1}}$ at 1 μm, taking into account that for any reasonable scenario of γ-ray production the differential intrinsic spectrum of γ-rays hardly could be flatter than $\mathrm{d}N/\mathrm{d}E \propto E^{-1}$. This estimate agrees, within statistical and systematic uncertainties, with recent reports about tentative detections of the CIB at 2.2 and 3.5 μm by the Diffuse Infrared Background Experiment (DIRBE), as well as with the measurements of the background radiation at optical wavelengths from absolute photometry. The high flux of CIB at $\leq$ few μm wavelengths implies a significant distortion of the shape of the initial (source) spectrum of γ-rays from Mkn 501 at sub-TeV energies. The "reconstructed" intrinsic γ-ray spectrum shows a distinct peak in the Spectral Energy Distribution (SED) around 2 TeV with a flux by a factor of 3 higher than the measured flux. The energy spectrum of gamma radiation from both sides of the peak has power-law behavior with photon index $\alpha \simeq 1.5$ below 2 TeV, and $\alpha \simeq 2.5$ above 2 TeV. This agrees with predictions of SSC model. We also discuss the impact of the intergalactic absorption effect in derivation of the SSC parameters for the jet in Mkn 501.

Send offprint requests to: C. Renault (rcecile@in2p3.fr)

Key words: galaxies: BL Lacertae objects: individual: Mkn 501 – cosmology: diffuse radiation – infrared: general – gamma rays: observations – X-rays: galaxies

1. Introduction

The Cosmic Infrared Background (CIB) is contributed mostly by the red-shifted 'stellar' and 'dust' radiation components, and therefore carries vital cosmological information about the epoch of galaxy formation and their evolution in time. The derivation of information about CIB from direct measurements is a hard task which requires an effective removal of heavy contamination caused by foregrounds of different origin, in particular by the zodiacal light, stellar and interstellar emission of our Galaxy, etc (Arendt et al. 1998; Kelsall et al. 1998). The conclusions of this approach in the near-infrared domain are to a large extent model-dependent because they are generally based on comprehensive modeling of the foregrounds; the far-infrared background is determined with a better accuracy as it dominates the foreground emission (Hauser et al. 1998).

Very High Energy (VHE) γ-ray astronomy provides an independent and complementary approach for the study of the CIB. The idea is simple, and based on the detection of absorption features in the γ-ray spectra of distant extragalactic objects caused by interactions of VHE γ-rays with the CIB photons in their way from a source to the observer (Nikishov 1962; Gould & Schreder 1967; Stecker et al. 1992). The recent detections of γ-rays from two BL Lac objects, Mkn 421 and Mkn 501, with spectra extending up to 10 TeV and beyond, open an interesting path for the realization of this exciting cosmological aspect of VHE gamma-ray astronomy. Obviously, the success of the 'γ-astronomical' approach essentially depends on two crucial conditions: (i) accurate γ-ray spectrometry, and (ii) good understanding of the intrinsic (source) spectra of TeV γ-rays.

The observations of Mkn 501, the second closest X-ray selected BL Lac object with a redshift $z \simeq 0.034$, during its extraordinary outburst in 1997 yielded unique data, which initiated important theoretical studies of the physical conditions in the relativistic jets of BL Lac objects (see e.g. Tavecchio et al. 1998 (hereafter TMG); Kirk & Mastichiadis 1999, Hillas 1999; Coppi & Aharonian 1999a, Bednarek & Protheroe 1999, Krawczyn-

ski et al. 1999), as well as interesting efforts to set meaningful upper limits on the CIB flux (see Biller et al. 1998, Stanev & Franceschini 1998, Barrau 1998, Stecker & De Jager 1998, Stecker 1999, Aharonian et al. 1999, Coppi & Aharonian 1999b; Konopelko et al. 1999).

During the 1997 outburst, lasted several months, Mkn 501 showed dramatic variations of fluxes both in X-rays (BeppoSAX: Pian et al. 1998, RXTE: Lamer & Wagner 1998) and TeV γ-rays (Whipple: Catanese et al. 1997, Samuelson et al. 1998; HEGRA: Aharonian et al. 1997, 1999; Telescope Array: Hayashida et al. 1998; CAT: Djannati-Ataï et al. 1999). More importantly, the high TeV fluxes allowed monitoring of the energy spectrum of Mkn 501 on a diurnal basis, especially during very strong flares. On several occasions truly simultaneous observations of Mkn 501 were available in TeV and X-ray band (Krawczynski et al. 1999). A special interest presents the famous April 16, 1997 flare which was observed by BeppoSAX (Pian et al. 1998) and low-energy threshold ($\sim 300\,\mathrm{GeV}$) Whipple and CAT atmospheric Cherenkov telescopes (Catanese et al. 1997; Djannati-Ataï et al. 1999). Because of very large fluxes, the energy spectrum of the flare was obtained with good accuracy in broad dynamical ranges in both X-ray (0.1–100 keV) and TeV γ-ray (0.3–10 TeV) regimes. Within today's most popular, the so-called synchrotron-self-Compton (SSC) model of non-thermal high energy radiation of Mkn 501, the data of April 16, 1997 flare allow us to compute the intrinsic source spectrum of γ-rays. This information, coupled with almost simultaneous spectral measurements of γ-radiation by CAT, provides a good opportunity to analyze the intergalactic absorption signature in the observed VHE γ-ray spectrum.

Since the optical depth $\tau_{\gamma\gamma}$ of γ-rays in the intergalactic medium increases with energy (for any reasonable spectral shape of the CIB), most stringent constraints on the CIB come from the very energetic tail of the γ-ray spectrum of Mkn 501. For $E \geq 10$ TeV the $\gamma - \gamma$ absorption is dominated by the 'dust' component of CIB at far infrared (FIR) wavelengths, $\lambda \geq 10\ \mu\mathrm{m}$. Therefore, it is generally believed that a deep probe of CIB at optical and near-infrared (NIR) wavelengths is contingent only upon the discovery of more distant (e.g. with $z \geq 0.1$) VHE γ-ray sources. In this paper, however, we show that the accurate measurements of the spectrum of Mkn 501 by CAT at sub-TeV energies already provide meaningful upper limits on the CIB flux at wavelengths between 0.4 and a few $\mu\mathrm{m}$. Moreover, the analysis of the X-ray and γ-ray spectra of the April 16, 1997 flare within the homogeneous SSC model allows rather conclusive estimates of the CIB flux at such short wavelengths. The CIB flux $\lambda F_\lambda \sim 5$–$35\,\mathrm{nW\ m^{-2}sr^{-1}}$ at $\lambda \sim 1\ \mu\mathrm{m}$ gives a reasonable slope, $\nu F_\nu \propto E^{0.5}$, in the 'reconstructed' Spectral Energy Distribution (SED) of γ-rays at low energies - as expected within the framework of the SSC model. The significant intergalactic absorption of sub-TeV γ-rays leads to both the shift of the position ($E \simeq 2\,\mathrm{TeV}$) and increase of the flux ($\nu F_\nu \simeq 10^{-9}\,\mathrm{erg\ cm^{-2}\ s^{-1}}$) of the so-called Compton peak in the γ-ray spectrum. An analytical approach has been recently proposed by (TMG) for derivation of constraints on the jet parameters of TeV blazars. With these revised spectral parameters, new results in a well defined self-consistent SSC parameter-space for the jet of Mkn 501 in the high state are obtained.

2. Intergalactic absorption of VHE gamma rays

If we ignore the appearance of second-generation γ-ray photons in the source direction[1], the extinction of gamma radiation is reduced to a simple absorption effect, described by an energy dependent optical depth:

$$J_{obs}(E) = J_0(E)\ \exp\left[-\tau_{\gamma\gamma}(E)\right]$$

where J_0 and J_{obs} are the intrinsic (source) and detected γ-ray fluxes, respectively. In order to calculate the optical depth for γ-rays from several hundred GeV to 20 TeV (the typical energy range of current Cherenkov telescopes), one needs to know the distance to the source $d = c\,z/H_0$, where H_0 is the Hubble constant, and the flux of the diffuse background in a rather broad interval from sub-micron to 100 μm wavelengths (for close sources, $z \ll 1$, the CIB flux is independent of z). Note that if, for a given redshift z, the uncertainty in the estimate of the distance to the source does not exceed a factor of 1.5 (the current estimate of the Hubble constant H_0 is between 50 and 75 km/s/Mpc), the uncertainty connected with the CIB flux (directly measured and/or predicted by different cosmological models) is significantly larger. However, since in the method described below we intend to obtain *independently* the density of the CIB using the γ-ray data, we need to know the spectral shape (or possible shapes) of the CIB, rather than the absolute value of the CIB, in a broad band of wavelengths from 0.3 $\mu\mathrm{m}$ to 100 $\mu\mathrm{m}$.

2.1. CIB models

The calculations of CIB present a serious theoretical challenge because they require a complex treatment of number of cosmological assumptions and key physical processes of galaxy formation (see e.g. MacMinn & Primack 1996; Salamon & Stecker 1998, Madau & Pozzetti1999, Primack et al. 1999). It is important for our further discussion that most of cosmological models give rather similar shapes of the basic, the 'stellar' and 'dust' components of radiation - two distinct bumps at 1–2 $\mu\mathrm{m}$ and 100–200 $\mu\mathrm{m}$ (see e.g. Dwek et al. 1998; Primack et al. 1999). The shape (the precise position, depth and width) of the mid-infrared 'valley' contains more uncertainties because of the lack

[1] This is a good approximation unless the intergalactic magnetic field $B \ll 10^{-16}$ G. In the case of such extremely small intergalactic magnetic fields, the new generation (cascade) γ-rays, produced by secondary electrons and positrons via inverse Compton scattering on 2.7 K microwave background, remain in the field of view of the detector and arrive almost simultaneously with the primary γ-rays. If so, the cascade spectrum could dominate over the primary γ-ray spectrum, and therefore instead of the absorption features in the primary spectrum, we should detect a standard power-law ($\propto E^{-1.5}$) cascade spectrum with exponential cutoff at E^*, determined from the condition $\tau(E^*) = 1$.

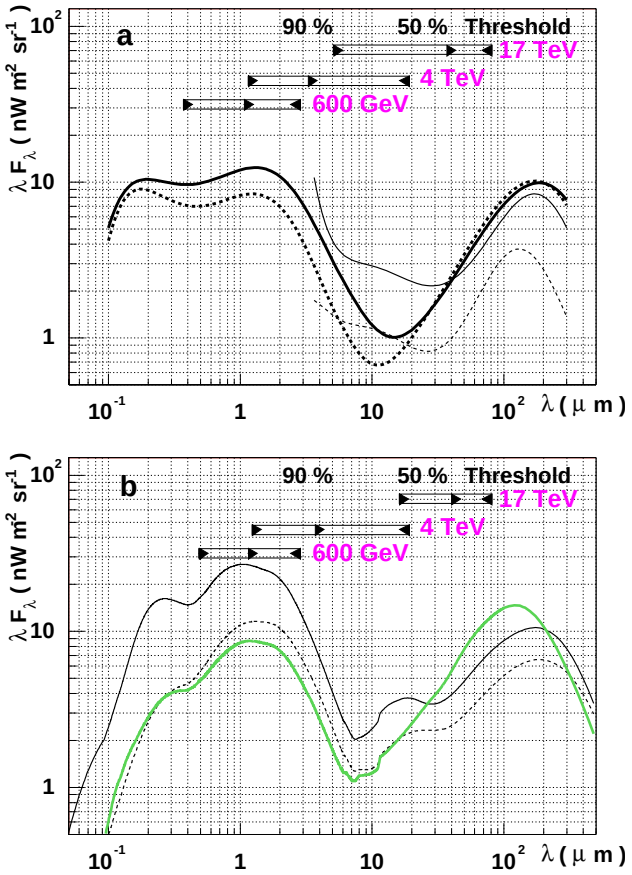

Fig. 1a and b. Predictions for the CIB fluxes by different cosmological models. **a** the LCDM and CHDM models of Primack et al. (1999) are shown by thick solid and dashed lines, respectively. The maximum and minimum CIB fluxes from the model of Malkan and Stecker (1998) are shown by thin solid and dashed lines, respectively. The arrows show the wavelength intervals (from the threshold) of CIB photons with 50% and 90% contributions to the absorption of TeV γ-rays with energies 600 GeV, 4 TeV, and 17 TeV computed for the LCDM distribution. **b** three models discussed by Dwek et al. (1998) are drawn with solid line (PFI model), dashed (PFC model) and grey line (ED model). The arrows show the wavelength intervals computed for the ED distribution. The thresholds indicated by the left side of the arrows are independent of the CIB model.

of adequate information necessary for modeling the radiation associated with warm dust component.

In this paper, we use a sample of recent models providing information from roughly 0.1 to 300 μm. The predictions of two such models, LCDM (Lambda Cold Dark Matter) and CHDM (Cold and Hot Dark Matter) suggested by Primack et al. (1999) for the density of CIB is shown in Fig. 1 (top panel). For comparison we show also the maximum and minimum CIB fluxes derived phenomenologically by Malkan & Stecker (1998) for wavelengths $\lambda \geq 3.5\,\mu$m. However, in this paper we are primarily interested in absorption of low energy, $E \leq 2\,\mathrm{TeV}$ γ-rays, which effectively interact with NIR background photons. Therefore below we will not use the CIB models of Malkan & Stecker (1998).

In the bottom panel we present another three CIB models suggested by Dwek et al. (1998) which differ from each other by cosmic star formation histories. The PFI and PFC models are based on different chemical evolution scenarios directly related to the star formation rate based on the Pei & Fall (1995) calculations. The ED model (Extragalactic DIRBE results) is derived from UV and optical observations and reproduce the COBE fluxes (for details see Dwek et al. 1998).

The flux dispersion between the curves in Fig. 1 shows that neither the shape nor the intensity can be precisely predicted by current CIB models. Actually in our approach we intend to "measure" the CIB density ourselves. Therefore we are interested in the shape rather than in the absolute flux predicted by CIB models. Fortunately, in the most informative parts of the gamma-ray spectrum, namely below 1 TeV and above 10 TeV, the absorption of γ-rays from relatively nearby BL Lac object Mkn 501 is contributed mainly by two well separated parts of the CIB spectrum - $\lambda \leq$ few μm and $\lambda \geq 10$ μm, respectively. This allows us to introduce a scaling factor SF, which does not change the shape, but varies the absolute flux of CIB within reasonable limits, and thus to derive the "best-fit" values or upper limits on SF for each specific CIB model.

2.2. $\gamma - \gamma$ pair production

A γ-ray photon with energy E penetrating through an isotropic field of photons, can interact with any background photon of energy $\epsilon \geq \epsilon_{th} = (m_e c^2)^2/E \simeq 0.26\,(E/1\,\mathrm{TeV})^{-1}\,\mathrm{eV}$. Since the cross-section of the pair production $\gamma\gamma \rightarrow e^+e^-$ peaks at $\epsilon_{max} \simeq 4\epsilon_{th}$ with $\sigma_{\gamma\gamma} \simeq 10^{-25}\,\mathrm{cm}^2$ (see e.g. Herterich 1974), for a large class of relatively flat and smooth (e.g. power-law) spectra of the field photons, approximately half of the optical depth $\tau_{\gamma\gamma}$ is contributed by a rather narrow band of the background radiation within $\epsilon_{max} \pm 1/2\epsilon_{max}$. For a more realistic shape of the CIB photons with two distinct bumps at NIR and FIR, the relative contributions of different parts of the spectrum of CIB do not follow this simple relation. In Fig. 1, we show the energy intervals from the threshold ϵ_{th} of CIB photons contributing to the 50% and 90% of the optical depth of intergalactic absorption calculated for the LCDM and the ED type CIB spectra for 3 energies of primary γ-rays: E =600 GeV, 4 TeV, and 17 TeV. It is seen that 50% of absorption of 600 GeV γ-rays is caused by a narrow band of CIB between 1–3 μm, while the remaining contribution comes essentially from the 0.4–1 μm band for the LCDM model. The thresholds depends only on the TeV photon energy, so they are independent of the CIB model. The bands are significantly narrower for the ED model because both NIR and FIR parts are more "peaked".

The absorption of multi-TeV γ-rays is equally contributed both from mid- and far-IR parts of the spectrum. So conclusions based on the absorption of these energetic γ-rays depend strongly on the model of the CIB, first of all on the depth of the mid-IR 'valley' of the CIB. It is important to note that conclusions concerning the change of the spectral shape of sub-TeV γ-rays due to the CIB absorption is independent of the density of

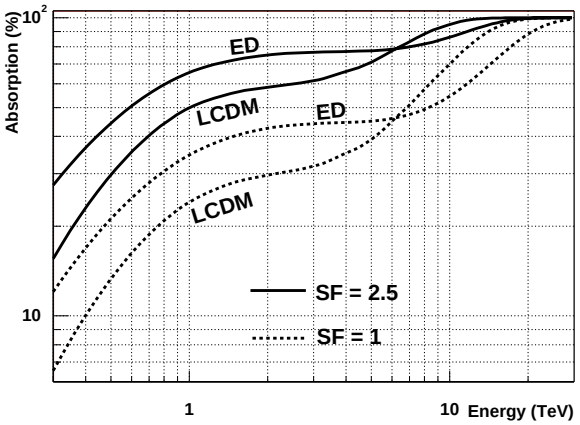

Fig. 2. Absorption in percents of γ-rays from Mkn 501 in function of the gamma energy calculated for two different scaling factors (1 and 2.5) and two models (LCDM and ED).

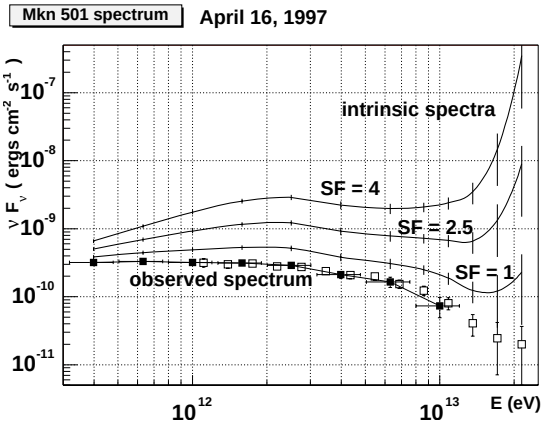

Fig. 3. Spectral energy distribution of γ-rays from Mkn 501 as detected by CAT during the April 16, 1997 flare (filled squares). The spectral points of the HEGRA 'time-averaged' spectrum normalized to the CAT flux at 1 TeV are also presented (open squares). Statistical errors only are shown. Three intrinsic γ-ray spectra are computed using the LCDM model and scaling factors of 1, 2.5 and 4.

mid- and far-IR photons, these photons being beyond the $\gamma - \gamma$ interaction threshold.

The optical depth is a function of the γ photon energy E defined as, for a source at a redshift $z_s \ll 1$:

$$\tau(E) = \frac{cz_s}{H_0} \int_{-1}^{1} \frac{1 - cos\theta}{2} d(cos\theta) \int_{\epsilon_t}^{\infty} n(\epsilon)\sigma(E, \epsilon, \theta) d\epsilon$$

where θ is the angle between both photons, ϵ the IR photon energy and $\sigma(E, \epsilon, \theta)$ is the pair-production cross-section.

In Fig. 2 we present the portion (percentage) of absorbed γ-rays, $P = 1 - \exp[-\tau_{\gamma\gamma}(E)]$, from Mkn 501 for the LCDM and ED models assuming two different scaling factors: $SF = 1$ and 2.5. Hereafter all calculations are performed for the Hubble constant $H_0 = 60\,\mathrm{km/s\,Mpc}$.

3. Constraints on CIB

Given the lack of reliable information on the intrinsic γ-ray spectrum, an upper limit on the CIB flux could be derived by formulation of *a priori*, but astrophysically meaningful requirement on the shape of the spectrum of γ-rays produced in the source. In particular, we may require that within any reasonable model of γ-ray production, and for a given observed γ-ray spectrum $J_{obs}(E)$, the *source* spectrum, $J_0(E) = J_{obs}(E) \exp[\tau_{\gamma\gamma}(\mathrm{E})]$, should not contain, at any energy E, a strongly (e.g. exponentially) rising feature.

In Fig. 3 we show the spectrum of Mkn 501 as measured by the CAT telescope during the strong April 16, 1997 flare in the energy region from 300 GeV to 12 TeV (statistical errors only). Unfortunately, because of bad weather this remarkable flare could not be observed by the HEGRA telescope system. However, the HEGRA observations of Mkn 501 revealed that, despite dramatic flux variations in time-scales $\leq 1\,\mathrm{day}$, the shape of the energy spectrum above 1 TeV remained essentially stable throughout the entire state of source high activity in 1997. So we show the HEGRA 'time-averaged' spectrum (Aharonian et al. 1999) normalized to the CAT April 16, 1997 spectrum at $E = 1\,\mathrm{TeV}$ with the re-scaling factor of ≈2.2. At TeV energies the agreement between the CAT and HEGRA spectra is quite impressive. Below 1 TeV we show only the CAT spectral points since in this energy region both the statistical and systematic errors of the data obtained close to the energy threshold of the HEGRA telescope system are rather large. Moreover, the inclusion of the HEGRA 'time-averaged' spectral points at sub-TeV energies in Fig. 3 cannot be justified because of reported noticeable variation of the spectrum of Mkn 501 at such *low* energies in the time-scales $\leq 1\,\mathrm{day}$, especially during strong flares (Djannati-Ataï et al. 1999).

3.1. Limit on the CIB at FIR

More than half of the intergalactic absorption of highest energy photon above 10 TeV detected from Mkn 501 is contributed by interactions with the 'dust' component of CIB at wavelengths $\lambda \geq 10\,\mu\mathrm{m}$ (see Fig. 1). The optical depth increases with energy so rapidly that requiring the absorption-corrected spectrum to be concave is already sufficient to impose an interesting constraint on the CIB. Therefore the most robust upper limits on CIB at FIR are provided by the HEGRA data above 10 TeV. Indeed, in this energy region the source spectrum 'reconstruction factor' $\exp(\tau_{\gamma\gamma})$ should not exceed the exponential term of the observed spectrum of Mkn 501 which in the energy region up to 24 TeV is well described as $J_{obs}(E) \propto E^{-1.92} \exp(-E/6.2\,\mathrm{TeV})$ (Aharonian et al. 1999). The intrinsic (reconstructed) spectra of Mkn 501 are shown in Fig. 3 assuming that the spectral shape of CIB is described by the LCDM model with 3 different scaling factors: $SF = 1, 2.5$, and 4.

In order to obtain an upper limit on the CIB intensity around 50 μm, we require that the intrinsic flux at 17 TeV (the highest energy point in the HEGRA data set with adequate statistical significance; Aharonian et al. 1999) should not exceed the flux at 4 TeV. In the case of the SSC model this implies that for any reasonable combination of model parameters, the Comp-

Table 1. The 68 % C.L upper limits on the scaling factor SF derived at FIR from 20 to 80 μm for different CIB models.

Model	SF_{max}	Upper Limit at 20 μm	(nW m^{-2} sr^{-1}) at 80 μm
LCDM	3.4	3.6	21.1
CHDM	2.9	2.9	18.0
PFC	2.6	5.9	11.4
PFI	1.7	6.3	12.7
ED	1.15	2.9	14.2

ton peak should not appear at energies beyond several TeV (in particular, due to the Klein-Nishina effect). For the hadronic ("π^0-decay") models (e.g. Dar & Laor 1997) this implies that the spectrum of accelerated protons should not be flatter than the "nominal" E^{-2} spectrum.

It is seen from Fig. 3 that the LCDM type spectrum of CIB with scaling factor up to $SF = 2.5$ do not contradict this 'reasonable-source-spectrum' criterion. Actually, the acceptable range of SF at 68% C.L. extends to $SF = 3.4$ (see Table 1). Note that as the above formulated $\nu F_\nu(17\,\mathrm{TeV})/\nu \mathrm{F}_\nu(4\,\mathrm{TeV}) \leq 1$ criterion could be treated as a tight condition, the results presented in Table 1 are based on a rather relaxed, 68% C.L. statistical requirement.

The upper limits on SF are quite sensitive to the exact shape of the CIB spectrum because the absorption of 17 TeV γ-rays is contributed mostly by the background photons from the rising branch of the CIB spectrum ($\lambda \geq 10\ \mu$m, see Fig. 1), therefore the optical depth increases strongly with energy of γ-rays.

The results are summarized in Table 1. The derived values of $SF_{\max}$ give upper limits on the absolute flux of CIB from 20 to 80 μm shown in Fig. 5. Note that the CHDM, LCDM, and ED models have rather similar slopes between 20 and 80 μm (see Fig. 1). Therefore the upper limits on CIB corresponding to these three models are very close. The same is true for the PFI and PFC models. For that reason in Fig. 5 we show only upper limits on CIB flux corresponding to LCDM (black line) and PFI (grey line) models as representatives of these two group of models, respectively.

Finally we note that although the extrapolation of the FIR upper limits shown in Fig. 5 do not contradict the COBE measurements at $\lambda \geq 100\,\mu$m, the maximum energy of about 17 TeV reported from Mkn 501 with high statistical significance, is not sufficient to provide model-independent information about the CIB at wavelengths beyond 80 μm.

3.2. Limit on the CIB at NIR

At shorter wavelengths, $\lambda \leq 10\ \mu$m, the constraints on the CIB come mainly from data below 10 TeV. For a power-law spectrum of the CIB, $n(\epsilon) \propto \epsilon^{-\beta}$, the optical depth is proportional to $\tau_{\gamma\gamma} \propto E^{\beta-1}$ (see e.g. Gould & Schreder 1967). In the 2–10 μm side of the 'valley' the CIB, contributed mainly by the starlight, has a typical spectrum $\lambda F_\lambda \propto \lambda^\delta$ with $\delta \simeq -1$ (see e.g. Dwek et al. 1998; Primack et al. 1999), or $n_{CIB}(\epsilon) \propto \epsilon^{-1}$. Therefore the shape of the γ-ray spectrum at energies between 2 TeV and 10 TeV remains essentially unchanged ($\tau_{\gamma\gamma}(E) \simeq$ constant), although the absolute absorption effect could be very large. This effect is clearly seen in Fig. 2. It makes rather difficult to extract information about CIB based merely on the γ-ray data in the *intermediate* energy range of γ-rays between 2 and 10 TeV.

Essentially more information about the CIB is contained in *low* energy, $E \leq 1$–$2\,\mathrm{TeV}$ γ-rays, since in this energy region the absorption effect again becomes energy-dependent (see Fig. 2). For the redshift of Mkn 501, $z = 0.034$, the optical depth $\tau_{\gamma\gamma}$ at 500 GeV remains less than 1 for any reasonable assumption about the CIB at NIR. At 1–2 TeV the optical depth could be close or even exceed 1, if $SF \geq 2$. Therefore, a variation of the density of the CIB by the scaling factor SF from 1 to 4 could lead to dramatic (up to factor of 10) increase of the 'reconstructed' flux at 1–2 TeV, while at energies below 500 GeV the impact is still not very large (less than factor of 2). This implies that the slope of the γ-rays energy spectrum from Mkn 501 below 1 TeV is very sensitive to the level of the CIB flux at NIR. Therefore it can be used not only to constrain the CIB, but also to "measure" the CIB flux at wavelengths from 0.25 to few μm, provided that a reliable intrinsic γ-ray spectrum could be derived from multi-wavelength studies of the source. Note that the result is insensitive to the FIR density.

The April 16, 1997 flare of Mkn 501 is particularly well suited for this task because (i) the appropriate distance to the source of about 170 Mpc - *sufficiently* large to provide non-negligible (e.g. measurable absorption at $E \leq 1$ TeV), and at the same time *not too* large for strong suppression of TeV emission; (ii) the availability of high quality X-ray and sub-TeV γ-ray data obtained simultaneously by BeppoSAX and CAT, and (iii) the general belief that the TeV radiation of this source has a synchrotron-self-Compton origin (SSC). In the SSC scenario the TeV γ-rays and synchrotron X-rays in a broad band from 0.1 keV to $\geq 100\,\mathrm{keV}$ are produced by the same population of electrons accelerated in the relativistic jet with Doppler factor ≥ 10 (for a review see Sambruna 1999). If the SSC model works for this source, it is possible to robustly predict the intrinsic γ-ray spectrum based on the multi-wavelength observations during a strong flare of Mkn 501.

In this paper we do not intend to model the April 16, 1997 flare, but rather we use a few well known results from previous applications of the SSC model. Within this, for a realistic set of parameters characterizing the synchrotron X-ray and inverse-Compton (IC) γ-ray emitting jet, the γ-ray photons with energy $\leq 1\,TeV$ or so are produced in the Thomson regime, and therefore are described by the same spectral index as the X-rays do below the so-called break (see e.g. Tavecchio et al. 1998). The spectrum of X-rays of April 16, 1997 flare measured by BeppoSAX (Pian et al. 1998) had a photon index 1.5 at 1 keV, and remained unusually hard up to very high energies with photon index 1.7 at 100 keV. Although for more definite conclusions one needs comprehensive modeling of the flare in a broad frequency band, we suppose that the sub-TeV γ-ray spectrum should repeat the spectral shape of relatively low energy X-rays, so we expect

a photon index of intrinsic spectrum of sub-TeV γ-rays close to 1.5 (see e.g. Krawczynski et al. 1999 for more general discussion). Another characteristic feature of the γ-ray spectrum is its so-called 'Compton peak' which unavoidably appears in any SSC or, more generally, external radiation Compton models (see e.g. Sikora et al. 1997).

The spectrum of the IC γ-rays in a broad energy band, including the transition region from the Thomson regime to the Klein-Nishina regime (which is around 1 TeV here), has a rather complicated form. For convenience, following the recommendation of Sikora et al. (1997), we fit the γ-ray spectrum, corrected for the intergalactic absorption with a given scaling factor SF, on the $(log(\nu F(\nu)), log(E))$ plane by a parabola with a slope at 600 GeV α_{600} (photon index).

The relation between SF and α_{600} computed by χ^2 minimization is shown in Fig. 4. These results imply that the photon index expected around 1.5 within SSC model for the 'Thomson' branch of the IC spectrum could be achieved for a scaling factor SF ranging between 0.5 and 2.8 at 99% CL (LCDM model). This implies a CIB flux of ≈5–35 nW m^{-2} sr^{-1} at 1 μm. The analogous calculations for each of the other four CIB models lead to the limits summarized in Table 2. Remarkably, the difference between the results derived for different models is always less than 20–30%. Thus the conclusion about the lower and upper limits of variation of the CIB intensity at 1 μm, allowed by the SSC model, is very robust.

The above estimate of the CIB flux is based on a model-assumption that the observed sub-TeV γ-rays are produced within the framework of the SSC model as a result of inverse Compton scattering of highest energy electrons responsible also for the synchrotron radiation of the jet. However, the strong relation between the scaling factor SF and the photon index of the intrinsic sub-TeV γ-ray spectrum allows very robust constraint on the CIB without a specific model assumption. Indeed from Fig. 4 follows that at large scaling factor SF, the 'reconstructed' γ-ray spectrum becomes extremely hard, e.g. with $\alpha_{600} \leq 1$ for $SF \approx 5$. Such spectrum seems to be unacceptably hard for any realistic scenario of γ-ray production connected with either protons or electrons. So we may draw a conclusion that at $99\,\%$ C.L. the value $\simeq 60$ nW/m^2 sr should be considered as an absolute upper limit on the CIB flux at 1 μm. An assumption of a smaller distance to Mkn 501, e.g. adopting for the Hubble constant H_0=75 km.Mpc^{-1}.s^{-1} (instead of 60 km.Mpc^{-1}.s^{-1}), could soften this upper limit only by $25\,\%$.

In Fig. 5 we compare the limits on the CIB intensity derived above with the direct measurements. Results obtained in this paper are shown by large horizontal bars corresponding to the energy range of CIB photons which can interact with 600 GeV photons. The 99% CL limits correspond to the 5 different CIB models. The upper limit at 60 nW m^{-2} sr^{-1} assumes a differential source spectrum softer than E^{-1}. The allowed range of variation of the CIB between 5 and 35 nW m^{-2} sr^{-1} is derived assuming inverse Compton origin of TeV radiation of Mkn 501. These results are in good agreement with recently reported fluxes of CIB at 2.2 μm and 3.5 μm based on the DIRBE measurements (Dwek & Arendt 1998, Gorjian et al. 1999), as well with the measurement of the background radiation from absolute photometry (Bernstein et al. 1999).

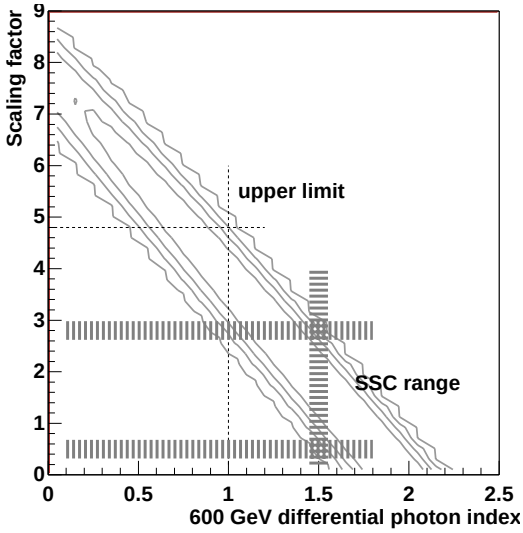

Fig. 4. Relation between the scaling factor SF and the photon index of the γ-ray spectrum after correction for absorption in the CIB, α_{600}, obtained from the χ^2 fit for the LCDM model. The contour levels are at 10, 90 and 99 % C.L.; the scaling factor related to the upper limit is the maximum scaling factor compatible at 99 % C.L. with $\alpha_{600} = 1$ while the scaling factors allowed by the SSC model lie between the minimum and the maximum scaling factors compatible at 99 % C.L. with $\alpha_{600} = 1.5$.

Table 2. The upper limit on the CIB based on the assumption that the differential source spectrum of γ-rays at sub-TeV energies is softer than E^{-1}, and the interval of CIB densities allowed by the SSC model of TeV radiation of Mkn 501. The 99 % C.L. limits are relevant to the NIR wavelengths from 0.4 to 3 μm, corresponding to the energy range of interaction for 600 GeV photons.

Model	Upper Limit nW m^{-2} sr^{-1}	SSC limits nW m^{-2} sr^{-1}
LCDM	48	5 to 28
CHDM	60	7 to 34
ED	51	7 to 30
PFC	44	5 to 26
PFI	57	6 to 34

4. Impact of the CIB flux on the jet parameter-space of Mkn 501

The analysis of the spectral shape and variability of the synchrotron and IC components of non-thermal radiation of TeV blazars within the framework of a single-zone SSC model may yield important constraints in the parameter-space of the X-ray and γ-ray production region (see e.g. TMG, Bednarek & Protheroe 1999). Among the key observables used in derivation of constraints on the jet parameters are the frequency ν_{IC} and

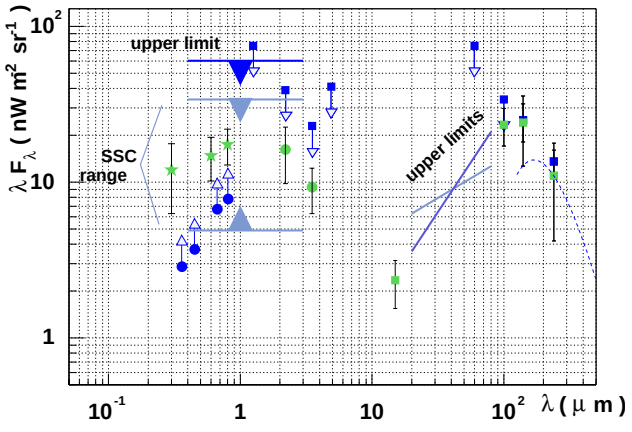

Fig. 5. CIB spectral energy distribution. The results of this paper are represented by large bars (0.4–3 μm, 99% CL) and are valid for all reasonable models or the SSC model (grey bars). Two limits are plotted in the range 20–80 μm (68% CL) as the results depend on the CIB slope. See text for details. The DIRBE results are shown by black squares (Hauser et al. 1998). Three grey squares correspond to CIB density extracted from WHAM H_α survey and Leiden/Dwingeloo HI data at 100, 140 and 240 μm (Lagache et al. 1999). The grey square at 15 μm comes from galaxies counting (Elbaz et al. 1998). The two grey dots show the fluxes of 2.2 and 3.5 μm (Dwek & Arendt 1998, Gorjian et al. 1999). The lower limits correspond to the Hubble Deep Field galaxy counts (Pozzetti et al. 1998), and the grey stars come from HDF results combined with ground-based spectrometry (Bernstein et al. 1999). The range of the CIB flux detected by FIRAS at very long wavelengths is shown by dotted line (Fixsen et al. 1998).

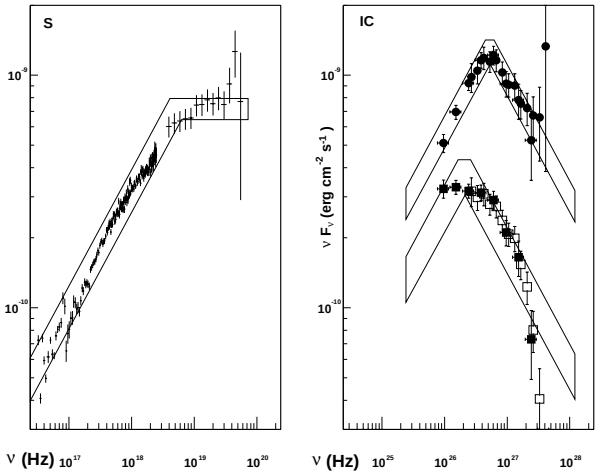

Fig. 6. Spectral energy distribution of the April 16, 1997 flare of Mkn 501. The X-ray data are from BeppoSAX observations (Pian et al. 1998). The γ-ray fluxes measured by CAT are shown by filled squares. The HEGRA 'time-averaged' spectral points obtained during the entire 1997 outburst of Mkn 501 (Aharonian et al. 1999) are also shown (open squares). Statistical errors only are drawn. The filled dots correspond to the CIB absorption-corrected fluxes computed for LCDM model ($SF = 2.5$). The 3 σ error boxes are used to model the spectra.

the *apparent* luminosity[2] $\nu_C L(\nu_{IC})$ of the Compton peak. Since the intergalactic absorption of γ-rays could significantly deform the original information about both parameters (see Fig. 6), we study the impact of the CIB density in the parameter-space of the jet in Mkn 501. For calculations, we use the convenient analytical approach recently developed by (TMG) for the homogeneous SSC model of TeV blazars. Detailed discussion of the SSC model is not the aim of this paper but rather we show the impact of the CIB absorption on the derivation of these parameters.

4.1. Model parameters and observables

The homogeneous SSC model describes the emission of electrons in a single blob with three basic model parameters: the radius R, magnetic field B, and Doppler factor of the bulk motion δ of the blob. An important information about the ratio R/δ is contained in the observed source variability time-scale t_{var}, namely the radius of the source should not exceed $R_{max} = t_{var} \times c \times \delta$. Thus the constraints in the parameter-space for the given maximum size (defined through the variability time-scale) can be expressed in terms of two parameters on the $(\log B, \log \delta)$ plane.

[2] Below for convenience we use the *apparent* luminosity of the source which is defined as the luminosity of an isotropically emitting source at a given distance. The intrinsic luminosity of the blob relativistically moving towards the observer with Doppler factor $\delta \gg 1$ is much ($\propto \delta^4$) smaller.

A distinct feature of the SSC model is the characteristic SED of radiation with two pronounced, synchrotron and Compton bumps which, in the case of X-ray selected BL Lac population, appear in the X-ray and the TeV γ-ray bands respectively (see e.g. Ulrich et al. 1997). The observations of X-rays require a population of relativistic electrons with power-law spectrum broken at energy γ_b. The specific values of the indices are determined by the spectral shape of the synchrotron radiation below and above the synchrotron peak.

In the quiescent state, the synchrotron radiation of Mkn 501 is characterized by a synchrotron peak at $\nu_s \simeq 10^{16}$ Hz, and spectral indices $\alpha_1 = 0.5$ and $\alpha_2 = 1.75$ (TMG). During the April 16, 1997 flare the X-ray spectrum was exceptionally hard with photon index less than 2 at least up to 100 keV, indicating a dramatic shift of the synchrotron peak by at least two orders of magnitude (Pian et al. 1998). Due to the lack of statistics, both the exact position for the synchrotron peak position and the synchrotron luminosity during the April 16, flare are not well defined.

The synchrotron spectrum of Mkn 501 in the high state is represented in the form of broken power-law with spectral indices $\alpha_1 = 0.5$ and $\alpha_2 = 1$ below and above the energy $h\nu_b = 21.5\,\mathrm{keV}$ ($\nu_b = 5.2 \pm 0.3 \times 10^{18}$ Hz (see Fig. 6). Additionally, we assume a high energy cutoff at 300 keV, which naturally could be attributed to the cutoff in the acceleration spectrum of electrons. The index α_2 as well as the position of the cutoff are rather qualitative, but fortunately the final conclusions do not depend strongly of their exact values. The total luminosity is then $\nu_s L(\nu_s)$=2.5±0.1 10^{45} erg.s^{-1}.

According to the TMG description, the IC peak should be represented by a broken power-law with the same spectral index $\alpha_1 = 0.5$ before the maximum and the spectral index $\alpha_2 = 1.5$

Table 3. The parameter ν_{IC} (in units 10^{26} Hz), $\nu_{IC}F(\nu_{IC})$ (in units 10^{-9} erg cm^{-2} s^{-1}), E_{ICmax} (in units 10^{12} eV) and $\nu_{IC}L(\nu_{IC})$ (in units 10^{45} erg s^{-1}) for two CIB models (LCDM and PFI) and two values for the scaling factor SF (1 and 2.5). The first line of the table corresponds to the γ-ray spectrum without intergalactic absorption.

Model	ν_{IC}	$\nu_{IC}F(\nu_{IC})$	E_{ICmax}	$\nu_{IC}L(\nu_{IC})$
no absorpt.	2.1±0.2	3.9±0.1	0.9±0.1	1.3±0.1
LCDM ×1	3.6±0.2	6.0±0.2	1.5±0.1	2.1±0.1
LCDM ×2.5	5.3±0.3	13.1±0.3	2.2±0.1	4.5±0.1
PFI ×1	4.5±0.2	9.4±0.2	1.9±0.1	3.2±0.1
PFI ×2.5	7.7±0.5	40.0±0.1	3.2±0.2	13.9±0.4

after, as shown in Fig. 6. The position of the maximum, and therefore the total energy depend on the assumption about the CIB absorption. Table 3 presents these observable parameters computed with no absorption and with the LCDM and PFI models, using SF=1 or 2.5.

It is interesting to note that the correction of the observed γ-ray spectrum for the intergalactic absorption, assuming typically a CIB flux at the level of 25 nW $^{-2}$ sr^{-1} at $\lambda \sim 1$ μm, results in a symmetric SED with a distinct maximum at 2 TeV, and power-law type behavior with spectral indices 0.5 and 1.5 below and above the peak, respectively, although we constrained *only* $\alpha_1 = 0.5$. This is a feature predicted by the SSC model for the IC radiation provided that the synchrotron X-radiation is described by a broken power-law with spectral indices $\alpha_1 = 0.5$ and $\alpha_2 = 1$ (TMG, Krawczynski et al. 1999).

4.2. The constraint regions on the ($\log B, \log \delta$) plane

TMG have suggested three independent constraints on allowed regions in the ($\log B, \log \delta$) plane based on (i) the positions of the synchrotron and Compton peak frequencies (area A), (ii) the synchrotron and Compton peak luminosities (area B), and (iii) the equilibrium between radiative cooling and escape of electrons (area C). It is important to note that the convenient approximate analytical formulae derived by TMG are applicable to the treatment of the IC scattering relativistic (Klein-Nishina) regime required here.

The first condition leads to the following simple relation between B and δ (Eq. 16) in TMG)[3]:

$$(A)\; B\,\delta_{10}^{-1} \approx 1.5 \frac{\nu_{s,19}}{\nu_{IC,26}^2} \qquad (1)$$

where B is in Gauss, $\delta_{10} = \delta/10$, $\nu_{s,19} = \nu_s/10^{19}$ Hz, and $\nu_{IC,26} = \nu_{IC}/10^{26}$ Hz.

The IC peak is very sensitive to the CIB absorption. Typically, the peak position shift by a factor 3 (up to 10) towards higher frequencies for the absorption-corrected spectrum. The total energy follow a similar evolution. This implies that the ignorance of the intergalactic γ-ray absorption would overestimate the B/δ ratio by a factor of up to 10 or even more. This is seen in Fig. 7 from comparison of the regions (A) on the top and bottom panels.

The comparison of the observed luminosities in the synchrotron and the IC peaks gives the second relation between the magnetic field and the Doppler factor (Eq. (22) in TMG)

$$(B)\; B\delta_{10}^{2.5} \geq 0.5\,(\nu_{s,19}\,\nu_{IC,26})^{-1/4}\,\frac{(\nu_s L(\nu_s))_{45}}{(\nu_{IC}L(\nu_{IC}))_{45}^{1/2}}\,t_{var,h}^{-1} \qquad (2)$$

where $(\nu_s L(\nu_s))_{45} = (\nu_s L(\nu_s))/10^{45}\,\mathrm{erg\ s^{-1}}$, $(\nu_{IC}L(\nu_{IC}))_{45} = (\nu_{IC}L(\nu_{IC}))/10^{45}\,\mathrm{erg\ s^{-1}}$ are the synchrotron and IC peak *apparent* luminosities and $t_{var,h} = t_{var}/1\,\mathrm{h}$ is the source variability time-scale. Here $t_{var,h}$=10 is assumed.

The region (B) shown in Fig. 7 is based on Eq. (2) with allowed ranges of uncertainties (3 σ) in the positions and total energies of the synchrotron and Compton peaks as described above. Also, it is interesting to note that the ignorance of the CIB absorption of γ-rays would lead to a conclusion that the radiative cooling of electrons in the jet is well dominated by synchrotron losses. This, however, could not be true, since after the correction of γ-ray fluxes for the intergalactic absorption, the IC luminosity in fact could be as high as (or even exceed) the synchrotron luminosity (see Fig. 6).

A relation between B and δ arises if one assumes that the break in the electron spectrum at γ_b is determined from the equilibrium between the cooling and escape from the source (obviously, there could be other reasons for the break in the electron spectrum, e.g. connected with the character of the acceleration mechanism). This model assumption leads to the following constraints in the Compton-cooling dominated regime (Eqs. (32) and (34) in TMG)[4]:

$$(C1)\; B\delta_{10}^{9} \geq 37.(\nu_s L(\nu_s)_{45})^2\,t_{var,h}^{-2}\,\beta_{esc}^{-2}\nu_{IC,26}^{-1} \qquad (3)$$

and synchrotron-cooling dominated regime:

$$(C2)\; B \geq 0.18\,\beta_{esc}^{1/2}(t_{var,h}\,\nu_{IC,26})^{-1/2} \qquad (4)$$

Here β_{esc} is the electron escape velocity in units of the speed of light, *i.e.* a parameter which describes the energy-independent escape time as $t_{esc} = \beta_{esc}\,R/c$. Following TMG, we allow a change of this rather uncertain parameter within limits from 1/3 to 1.

To avoid strong absorption of TeV photons inside the blob due to pair-production of γ-rays interacting with optical photons, a minimum value for δ can be computed; it is used to check the validity of the area defined by the intersection between (A), (B) and (C) regions. For the Compton peak luminosity, we obtain

$$(D)\; \delta > 6.6\left(\frac{L(\nu_s)_{26}}{t_{var,h}}\sqrt{\nu_{IC,26}\nu_{s,19}}\right)^{0.2} \qquad (5)$$

The impact of the intergalactic absorption of γ-rays on the constraints described by the regions (B), (C) and (D) is less dramatic than on the region (A). Nevertheless, as can be seen from

[3] Since we do not have here γ_{max}(=300 keV) $\gg \gamma_b$(=100 keV), the expression of $g(\alpha_1, \alpha_2)$ must be modified. $g(\alpha_1, \alpha_2) = exp(1/(\alpha_1 - 1) + 1/(2 * (\alpha_2 - \alpha_1)) * (1 - \sqrt{\gamma_b/\gamma_{max}})$

[4] There is a mis-print in the TMG paper. The exponent of δ in Eq. (34) should be $(6/(1-\alpha_1) - 3)$ instead of $(6/(1-\alpha_1))$.

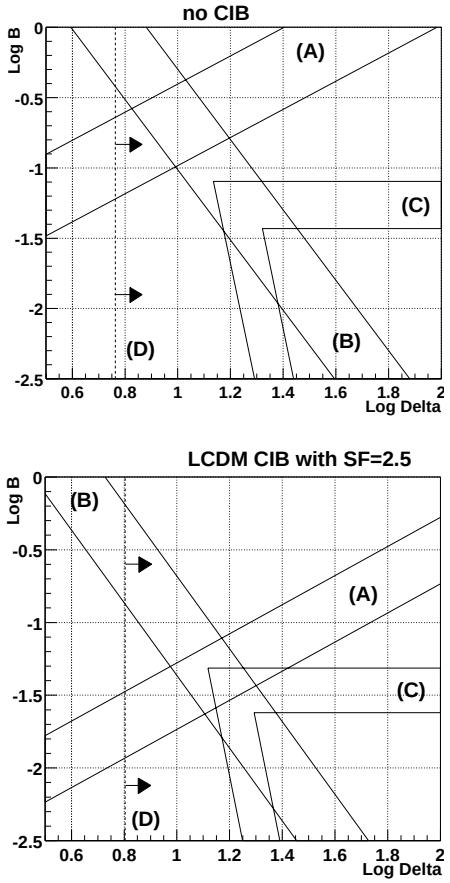

Fig. 7. Parameter-space for the April 16, 1997 flare of Mkn 501 (with t_{var}=10h) and SF= 0 (*i.e.* no intergalactic absorption) or $SF = 2.5$ for the LCDM model. See text for details on areas (A), (B), (C) and (D).

Fig. 7, even for these regions the effect is not negligible, and should be taken into account in any realistic attempt to constrain self-consistently the parameter-space in future studies based on detailed modeling of temporal and spectral characteristics of radiation. The scaling factor SF which determines effectively the flux of CIB at NIR, and therefore defines the level of distortion of γ-radiation in the sensitive region of the Compton peak, should be considered as a new free parameter in such studies.

Although the detailed modeling of radiation of Mkn 501 is beyond the framework of this paper, our study shows that the inclusion of the intergalactic absorption in the treatment results in a more consistent picture. In particular it moves the region (A) into the regions (B) and (C), and thus overcomes the incompatibility of different constraints on the principal model parameters. It is seen from Fig. 7 that after the correction of γ-ray fluxes for the intergalactic absorption, there is a trend for appearance of a compact *common* area for all three (A), (B), and (C) regions in the (log B,log δ) plane with magnetic field $B \simeq 0.05$ G, and Doppler factor $\delta \simeq 15$.

If the SSC model is confirmed in future studies, this would be also a strong evidence for the high CIB at NIR as is shown in Fig. 5, and used for the reconstruction of the source spectrum of the April 16, 1997 flare in Fig. 6. Such a high flux of CIB makes

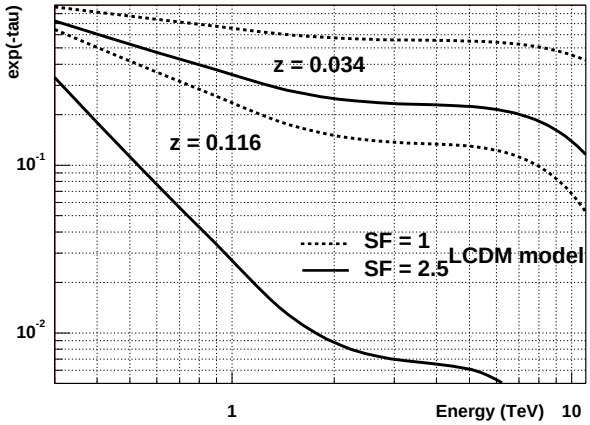

Fig. 8. Intergalactic absorption factor for Mkn 501 (z=0.034) and PKS 2155-304 (z=0.116) calculated for the LCDM model assuming two different scaling factors, $SF = 1$, and $SF = 2.5$.

significantly steeper ($\Delta\alpha \simeq 0.5$) the spectrum of sub-TeV radiation even from a relatively nearby source like Mkn 501. Obviously, the impact to the γ-ray emission from farther sources could be much stronger. In Fig. 8, the intergalactic absorption factor, $\exp(-\tau_{\gamma\gamma})$ is shown for Mkn 501 and for the BL Lac object PKS 2155-304 (z=0.116), which recently has been reported by the Durham group as a γ-ray emitter above 300 GeV (Chadwick et al. 1999). It is seen that for a high CIB flux with the scaling factor $SF = 2.5$ the γ-ray spectrum should suffer dramatic steepening ($\Delta\alpha \simeq 2$), before reaching the observer. Thus, even for a quite flat source spectrum, e.g. with photon index 1.5, we should expect very steep γ-ray spectrum from this source, ($\mathrm{d}N/\mathrm{d}E \propto E^{-3.5}$). Interestingly, at energies above 2 TeV the absorption becomes almost energy independent, therefore the observed spectrum essentially repeats the spectral shape of the source spectrum. However, the detection of $\geq 2\,\mathrm{TeV}$ radiation of γ-rays from PKS 2155-304 would be very difficult because of strong, by a factor of 100, suppression of γ-ray fluxes in that energy regime.

5. Summary

The accurate spectrometric observations of the γ-ray spectrum of Mkn 501 during the remarkable April 16, 1997 flare by the low-threshold imaging atmospheric Cherenkov telescope CAT in the energy region from 300 GeV to 10 TeV is used for extraction of important information about the CIB at wavelengths $\geq$ 0.4 μm. The interpretation of the spectrum of sub-TeV γ-rays, together with simultaneously obtained X-ray data of BeppoSAX, requires, within the one-zone SSC model, rather high NIR background at a level close to $20\,\mathrm{nW\,m^{-2}\,sr^{-1}}$ at 1 μm. Such high flux of CIB implies an essential distortion of the shape of the initial (source) spectrum of γ-rays from Mkn 501 not only at multi-TeV, but also at sub-TeV energies. The 'reconstructed' intrinsic γ-ray spectrum shows a distinct peak in the Spectral Energy Distribution around 2 TeV with a flux by a factor of 3 higher than the measured flux. Moreover, the energy spectrum of gamma radiation from both sides of the peak has power-

law behavior with spectral indices $\alpha \simeq 0.5$ below 2 TeV, and $\alpha \simeq 1.5$ above 2 TeV, which perfectly agrees with predictions of the SSC model. We have shown that the intergalactic absorption has non-negligible impact on the construction of self-consistent SSC parameters.

And finally, we argue that the CAT γ-ray data alone allow rather robust upper limits on the CIB, $\lambda F_\lambda \leq 60\,\mathrm{nW\,m^{-2}\,sr^{-1}}$ at 1 μm, taking into account that for any reasonable scenario of γ-ray production the differential intrinsic spectrum of γ-rays hardly could be flatter than $\mathrm{d}N/\mathrm{d}E \propto E^{-1}$.

Acknowledgements. We thank the referee, E. Dwek for his critical comments which help us to improve significantly the paper. We are grateful to E. Pian and H. Krawczynski who provided us with numerical values of BeppoSAX and HEGRA fluxes, as well as to J. Primack and J. Bullock for sending us the results of their numerical modeling of the CIB. We thank A. Barrau for fruitful discussions and F. Tavecchio for his help. F.A.A. thanks the LPNHE-Jussieu for kind hospitality during his stay at Université Paris VII.

References

Aharonian F.A., Akhperjanian A.G., Barrio J.A., et al., 1997, A&A 327, L5
Aharonian F.A., Akhperjanian A.G., Barrio J.A., et al., 1999, A&A 349, 11
Arendt R.G., Odegard N., Weiland J.L., et al., 1998, ApJ 508, 74
Barrau A., 1998, PhD Thesis, Université J. Fourier, Grenoble, France
Bednarek W., Protheroe R.J., 1999, MNRAS 302, 373
Bernstein R.A., Freedman W.L., Madore B.F., 1999, preprint
Biller S.D., Buckley J., Burdett A.. et al., 1998, PRL 80, 2992
Catanese M., Bradbury S.M., Breslin A.C., et al., 1997, ApJ 487, L143
Chadwick, PM., Lyons K., McComb T.J.L., et al., 1999, ApJ 513, 161
Coppi S., Aharonian F.A., 1999a, ApJ 521, L33
Coppi S., Aharonian F.A., 1999b, APh 11, 35
Dar A, Laor A., 1997, ApJ 478, 5
Djannati-Ataï A., Piron F., Barrau A., et al., 1999, A&A 350, 17
Dwek E., Arendt R.G., 1998, ApJ 508, L9
Dwek E., Arendt R.G., Hauser M.G., et al., 1998, ApJ 508, 106
Elbaz D., Aussel H., Césarsky C.J., et al., 1998, in: Cox P., Kessler M.F. (eds.), The Universe as seen by ISO, UNESCO, Paris: ESA Special Publications series (SP-427)
Fixsen D.J., Dwek E., Mather J.C., Bennett C.L., Shafer R.A., 1998, ApJ 508, 123
Gorjian V., Wright E.L., Chary R.R., 1999, astro-ph/9909428
Gould J., Schreder G., 1967, PR 155.5, 1404
Hauser M.G., Arendt R.G., Kelsall T. et al., 1998, ApJ 508, 25
Hayashida N., Hirasawa H., Ishikawa F., et al., 1998, ApJ 504, 71
Herterich, 1974, Nat 250, 311
Hillas A.M., 1999, APh 11, 27
Kelsall T., Weiland J.L., Franz B.A. et al., 1998, ApJ 508, 44
Kirk J.G., Mastichiadis A., 1999, APh 11, 45
Krawczynski H., Coppi P.S., Maccarone T., Aharonian F.A., 1999, A&A 353, 97
Konopelko A.K., Kirk J.G., Stecker F.W., Mastichiadis A., 1999, ApJ 518, L13
Lagache G., Haffner L.M., Reynolds R.J., Tufte S.L., 2000, A&A 354, L247
Lamer G., Wagner S.J., 1998, A&A 331, L13
MacMinn D., Primack J.R., 1996, SSRv 75, 413
Madau P., Pozzetti L., 1999, MNRAS 312 issue 2, L9
Malkan M.A., Stecker F.W., 1998, ApJ 496, 13
Nikishov A.I., 1962, Sov. Phys. JETP 14, 393
Pei Y.C., Fall S.M., 1995, ApJ 454, 69
Pian E., Vacanti G., Tagliaferri G., et al., 1998, ApJ 492, L17
Pozzetti L., Madau P., Zamorani G., Ferguson H.C., Bruzual A.G., 1998, MNRAS 298, 1133
Primack J.R., Bullock J.S., Somerville R.S., MacMinn D., 1999, AstroPart. 11 issue 1–2, 93
Salamon M.H., Stecker F.W., 1998, ApJ 493, 547
Sambruna R.M., 1999, IAUS 194, 113
Samuelson F.W., Biller S.D., Bond I.H., et al., 1998, ApJ 501, L17
Sikora M., Madejski G., Moderski R, Poutanen J., 1997, ApJ 484, 108
Stanev T., Franceschini A., 1998, ApJ 494, L159
Stecker F.W., De Jager O.C., Salomon M.H., 1992, ApJ 390L, L49
Stecker F.W., De Jager O.C., 1998, A&A 334, 85
Stecker F.W., 1999, APh 11 1–2, 83
Tavecchio F., Maraschi L., Ghisellini G., 1998, ApJ 509, 608
Ulrich M.H., Maraschi L., Urry C.M., 1997, ARA&A 35, 445 NASA ADS